Supporting Online Material for

Probing Transcription Factor Dynamics at the Single-Molecule Level in a Living Cell

Johan Elf, Gene-Wei Li, X. Sunney Xie*

*To whom correspondence should be addressed. E-mail: xie@chemistry.harvard.edu

Published 25 May 2007, *Science* **316**, 1191 (2007)
DOI: 10.1126/science.1141967

This PDF file includes:

Supplementary Online Material

1. Strain and plasmid construction

JE12, JE13, JE14

The strains were constructed using the suicide plasmid method described by Link *et al.* (*1*). A part of the *lacIOZ* region (*NC_000913*:364090-366734) was integrated in pKO3 resulting in pKO3-lacIOZ. The Venus(A206K) gene was amplified from a plasmid template using PCR primers (2A, 2B) and (2A, 3B) respectively. The fragments were cut with AseI and ligated into the AseI digested pKO3-lacIOZ, which resulted in plasmids pKO3-lacI:venusO121Z and pKO3-lacI:venusO123Z. These plasmids have the lacI:venus fusion with an O1 or O3 operator in the O3 position. The operators in positions O1 and O2 were removed from pKO3-lacI:venusO121Z using sequential PCR amplification and blunt end ligation using primers 4A, 4B and 5A, 5B. This resulted in plasmid pKO3-lacI:venusO001Z.

The plasmids pKO3-lacI:venusO121Z, pKO3-lacI:venusO123Z and pKO3-lacI:venusO001Z were used to create the *JE12, JE13, JE14* strains through homologous recombination with our wild type strain BW25993.

The A206K mutation, which makes Venus monomeric, was introduced in a *Venus* carrying plasmid by amplifying the plasmid using primers 6A, 6B.

Δ*lacI and* Δ*lacIOZ*

Deletions of *lacI* or the whole *lacIOZ* region of BW25993 were made by substituting selected chromosomal regions by a kanamycin cassette using the lambda Red recombinase method by Datsenko and Wanner (2000) (*2*). pKD20-carrying BW25993 was electroporated with Kanamycin cassettes amplified with primers 7A, 7B to make Δ*lacI*, and 7A, 8B to make Δ*lacIOZ.*

pJE15 and pJE17

The pJE15 and pJE17 plasmids were generated by Gateway LR reactions between pENTR/D/SD-lacI:venus or pENTR/D/SD-lacI(-41):venus and pVS167. pVS167 is a Gateway destination plasmid created with replication control from pET-COCO2(Novagene) and an arabinose inducable promotor from pBAD202 (Invitrogen). pENTR/D/SD-lacI:venus and pENTR/D/SD-lacI(-41):venus were created by directional topo-cloning in pENTR/D/SD (Invitrogen) of a PCR fragments amplified from *JE12* using primers (9A, 9B) and (10A, 9B).

Primers

2A CGATTCATTAATGCAGCTGGCACGACAGGTTTCCCGACTGATGGTGAGCAAGGGCGAGGAG
2B ACTCACATTAATTGTTATCCGCTCACAATTCCTTGTACAGCTCGTCCATGCCG
3B ACTCACATTAATTGCGTTGCGCTCACTGCCCCTTGTACAGCTCGTCCATGCCG
4A AGCTTAACCTTTAATGTTGATGAAAGCTGGCTACAGGAAG
4B ATAACAGCCCGTCGGATTCTCCGTGGGAAC
5A CAACAGCTAATTCACACAGGAAACAGCTATGACCATGA
5B GATTATACTACCACACAACATACGAGCCGGAAG
6A AAGCTGAGCAAAGACCCCAACGAGAAG
6B GGACTGGTAGCTCAGGTAGTGGTTGTC
7A GTGAATGTGAAACCAGTAACGTTATACGATGTCGCAGAGTGGCTGGAGCTGCTTCGAAGT
7B CCAACGCGCAGCCCGGACTCGGTAATGGCGCGCATTGCGCTGGGAATTAGCCATGGTCCA
8B GATTTGTGTAGTCGGTTTATGCAGCAACGAGACGTCACGGTGGGAATTAGCCATGGTCCA
9A CACCATGAAACCAGTAACGTTATACGATGTCG
9B TCACAATTCCTTGTACAGCTCGTCCA
10A CACCATGGCGGAGCTGAATTACATTCCC

2. LacI-Venus dimers *in vivo*

In order to determine whether the LacI-Venus fusion forms a dimer instead of a tetramer *in vivo*, we constructed an *E. coli* strain (*JE14*) with only one LacI dimer binding site (O1). The fluorescence intensity of the operator region is compared with that in *JE12*, which has two strong dimer binding sites (Fig S1 A). If the fusion protein binds to DNA as a tetramer, only one tetramer will be bound to the operator region in both *JE12* and *JE14*. However, if the fusion protein binds to DNA as a dimer, two dimers will be bound to *JE12*, whereas only one dimer can bind to *JE14*. We do not expect any significant binding to the O2 site in *JE12* since the binding constant is over 10 free monomers per cell (*3*). Figure S1 B shows that the fluorescence intensity is significantly higher in *JE12*, which suggests that our LacI-Venus fusion binds as a dimer when expressed at low concentration in *E. coli*.

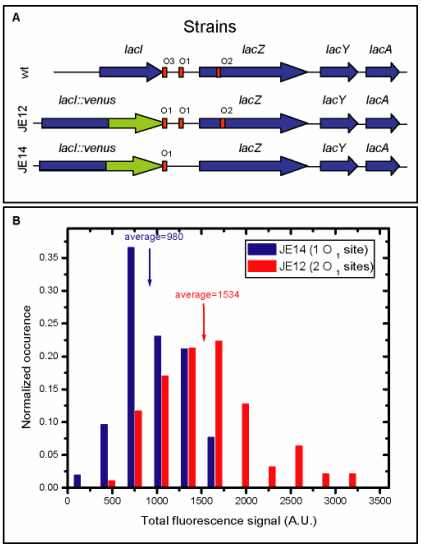

Fig. S1

3. Experimental set-up

Light source and microscope

The microscope system is composed of an Olympus IX71 inverted microscope frame, equipped with an ASI motorized XYZ stage, an Olympus PlanApo 60X 1.45 oil TIRFM objective, a thermoelectrically cooled (-50°C) EMCCD camera VersArray 1024 (Roper Scientific Inc), a narrow band pass excitation filter at 514/10 nm, a 525 nm LP Dichroic mirror and a combination of emission filters (545/35 nm and a 514nm notch filter). Excitation is controlled by a UniBlitz shutter. For short exposure times below 10ms, an acoustooptical modulator is used instead (described below). All the components are controlled by software (MetaMorph). A 2W Argon ion laser (Coherent Innova300) is used as the light source. The laser is spatially-filtered by a single mode fiber before entering the microscope.

Sample preparation

For microscope experiments, single colonies of the *JE12* (or *JE14*) strain were grown overnight in Media A (M9 media, 0.4% glucose, amino acids (MEM, Gibco) and vitamins (MEM, Gibco)). Overnight cultures were spun down and resuspended in an equal volume of Media A. This washing step was repeated twice. The cells were diluted 1:2000 in Media A and grown in a 37°C shaker for 4.5h. After 4.5h the OD_{600} was kept below 0.1 at all times by serial dilution 1:4 in pre-warmed media. All of the following steps, including microscopy, are performed at room temperature (*RT*) unless otherwise stated.

Before imaging, the bacteria were further concentrated ~50 times by a brief centrifugation and 5µl was applied in the center of a treated cover-slip surface described as below. Plastic Petri dishes with a glass cover-slip glued to a 14 mm hole at the bottom

(P35G-1.5-14-C, MatTek) were coated by poly-L-lysine (0.03%, Sigma) for 40 min and washed extensively in water. Poly-L-lysine is used to help immobilize bacteria at the bottom of the Petri dish. The bacteria were typically immobilized just a few minutes before the kinetic experiments.

Initial conditions for the induction and repression experiments are prepared differently. For induction experiments, 360 µl of Media A was first applied gently from the side of the 5 µl droplet. The liquid was contained as a large droplet within the cover-slip. For repression experiments, 20 µl of Media A with 100 µM IPTG was applied to the 5 µl bacterial droplet.

For the long time (20 min) response to IPTG shown in Fig. S2, media with different concentrations of IPTG was added to the 5 µl droplet on the poly-L-lysine coated cover-slip and the cells were incubated on the bench twenty minutes before imaging. Because of the conditions of incubation and because the number of both the *lac* permeases and *lac* repressors will change continually throughout the experiment, the response in Fig. S2 should not be considered a steady state response.

Induction and repression experiments:
For induction experiments the microscope was run in time-lapse mode where the control software acquires a 1 s (with laser intensity ~100 W cm^{-2}) fluorescence images every 10 s and then moves the stage to a region of unexposed cells in-between each image frame. Each image frame contains 50-100 bacteria. Induction is made by injecting 40 µl of x10 IPTG solution into the 360 µl droplet ~5 s after the first time-lapse image frame.

For the repression experiment, 1 ml of Media A with 1mM ONPF (Sigma) was added to the 20 µl 100 µM IPTG droplet at time zero. 1 s (with laser intensity ~100 W cm^{-2}) fluorescence images of the cells were taken at selected time points.

Western blot and Miller assay
Overnight cultures of the different strains were diluted 1:2000 and grown to OD_{600}~0.15 in M9 glucose with amino acids (MEM, Gibco) and vitamins (MEM, Gibco) at 37°C. Induced cells were grown with 1mM IPTG for 3h. These cells are used for both the western and Miller assays.

For western blot, proteins were separated on BioRad 12% SDS-PAGE minigels and transferred to a nitrocellulose membrane using standard protocols. The filter was blocked 1h in blocking buffer (dry milk in PBS+0.1% Tween20) , incubated with primary monoclonal LacI antibody (Upstate, 1:1000) for 2h, washed in blocking buffer, and incubated with secondary antibody (Molecular Probes, 1:2000 goat anti-mouse) for 1h. The filters were washed and imaged using ECL (Pierce).

The Miller assay was performed as described at
http://openwetware.org/wiki/Beta-Galactosidase_Assay_(A_better_Miller)

Stroboscopic single molecule tracking

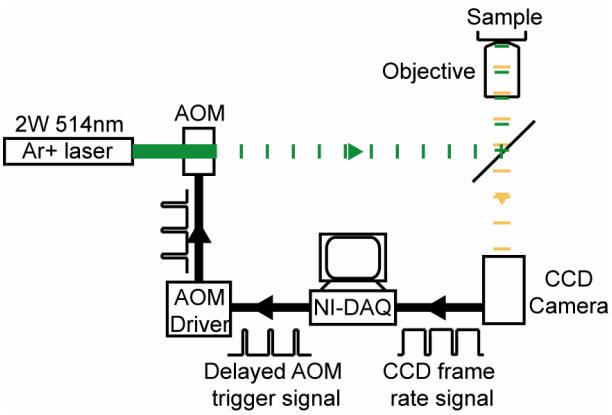

Fig. S5

To create short laser exposure for stroboscopic illumination, an acousto-optical modulator (40MHz, LiCONix) was placed in the laser beam path as a shutter (Fig. S5). A high-speed EMCCD camera (Cascade 512B, Photometrics) was used to achieve fast frame rates up to 100 frames/sec. The acousto-optical modulator is synchronized with the CCD frame rate through a Labview-based delay generator. At each frame the CCD controller triggers the Labview program, which then generates a delayed pulse with controllable delay time and pulse duration. The pulse train is fed into the AOM driver. In this way we created pulsed excitation that is synchronized with the camera.

4. Fluorescence Correlation Spectroscopy (FCS) experiment

Sample preparation

The LacI-Venus protein without DNA-binding domain was constructed by deleting the coding region corresponding to the 41 N-terminal amino acids. The truncated gene is expressed from pJE17 in Δ*lacIOZ*. Overnight grown bacteria are diluted 1:100 in media A and induced with 0.4% arabinose for 2h 20min. The bacteria are next washed, diluted 1:10 in Media A without arabinose and grown for an additional 120 min during which time the previously expressed proteins are diluted by cell division.

The Venus protein is similarly expressed from the low copy number plasmid. Cells expressing fluorescence proteins are prepared in plastic Petri dishes as described in previous sections.

in vivo FCS set-up

An Argon ion laser described in previous sections is used as excitation source. The beam is collimated before entering the microscope. The power is attenuated to 1 μW such that the intensity at the focus is about 700 W/cm^2.

An avalanche photodiode (APD) by Perkin-Elmer with 0.1 mm active area diameter was used as a detector for fluorescence correlation spectroscopy. The APD is mounted at the side port of an Olympus IX71 inverted microscope. A 50 mm planoconvex lens is used to further expand the image such that the projection of the diffraction-limited excitation spot in the image plane fills the active area of APD. The size of the detection volume is determined by recording fluorescence autocorrelation function of 10 nM Rhodamine dissolved in water under the same alignment. The estimated waist of detection volume is about w = 294 nm.

To monitor the positions of the cells and the excitation spot, a CCD camera (Cascade 512B, Photometrics) is mounted on the side port of the eyepiece. First the excitation profile is mapped by imaging concentrated Rhodamine solution. After the position of maximum intensity is recorded on the CCD, a Petri dish of cells is placed on stage and one cell is moved to the position of the excitation beam. We used the motorized stage to position the cell such that the excitation beam is at the center of the cell. After this procedure, the fluorescence signal is directed to the APD port. The fluorescence time trace and auto-correlation function is recorded by ALV-5000/E autocorrelation card. A typical correlation curve is obtained for 30sec acquisition.

Result

As shown in Fig. S6, the auto-correlation functions from individual cells expressing truncated LacI-Venus dimers are well-fit by the one-component diffusion model assuming a Gaussian detection volume ($C(t) = N^{-1}(1+4Dt/w^2)^{-1}$) (*4*). The average diffusion constant over five cells is $D_3 = 3 \pm 0.3 \mu m^2 s^{-1}$. Elowitz *et al.* have reported free diffusion constants of GFP in E. coli to be 7.7 $\mu m^2 s^{-1}$ (*5*). Considering the molecular weight of a LacI-Venus dimer is approximately six times larger than that of GFP, our measurement of diffusion constant falls into the expected range.

We also measured the diffusion constant of free Venus in *E. coli*. As shown in Fig. S7, the diffusion constant of free Venus is estimated to be $D_3 = 8^{+4}_{-2} \mu m^2 s^{-1}$. This is also in good agreement with Elowitz *et al*. (*5*).

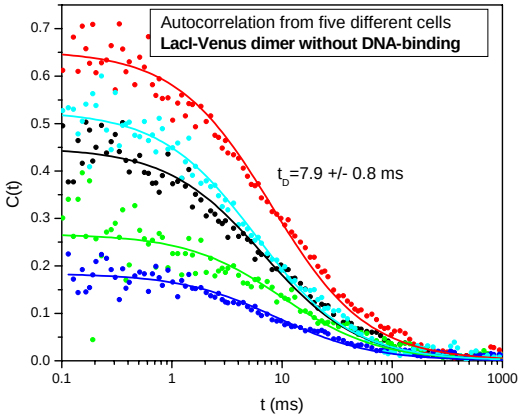

Fig. S6

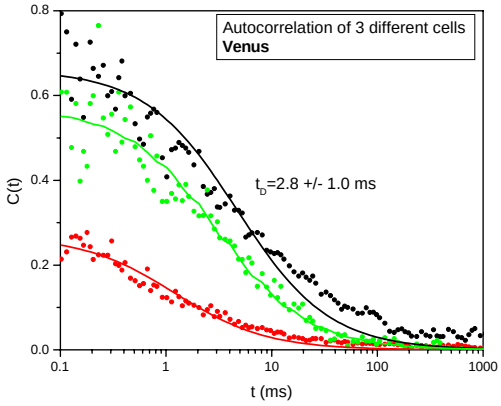

Fig. S7

5. *in vitro* sliding on flow stretched DNA

Methods

The *in vitro* assay was based on the method described by Blainey *et al.* (*6*). Briefly, one end of individual λ DNA was tethered on a coverslip coated as described in ref. *(6)*. The DNA was stretched by a constant laminar flow of buffer. Single LacI-Venus dimers that bind to the tethered DNA were imaged by a total internal reflection fluorescence microscope (TIRFM). A Cascade 512B CCD camera was used to record the location of the diffusing molecules at a rate of 10 Hz. A 514 nm Argon ion laser was used as the illumination source.

The buffer in the flow-stretch assay contains 40 pM of purified LacI-Venus molecules, 20% glycerol, 2 mM NaCl, 10 mM phosphate, 0.05 mM EDTA, 0.01% Tween, 0.5 mg/ml BSA, and 1 mM BME at a final pH ~7.3.

Results

We recorded 17 trajectories of individual LacI-Venus diffusing along DNA (Fig. S8 A). Each trajectory lasts 4-15 frames before the molecule is photobleached. The displacement histogram at 100ms interval is shown in Fig. S8 B. We calculate the diffusion constant from the trajectories to be $D_1 = 0.046 \pm 0.01 \mu m^2 s^{-1}$, or equivalently, $D_1 = (4.0 \pm 0.9) \times 10^5 bp^2 s^{-1}$ (Fig. S8 C). It should be noted that, at 2 mM salt concentration, the TF's residence time on the nonspecific DNA sequence is significantly longer than that measured *in vivo*. This allows us to detect its diffusion over hundreds of milliseconds.

Recently, Wang *et al.* measured the 1D diffusion constant of LacI dimers with a GFP fusion to the N-terminal domain of LacI using a different method (*7*). Our measurement is within the range of the diffusion constants reported by Wang *et al.*

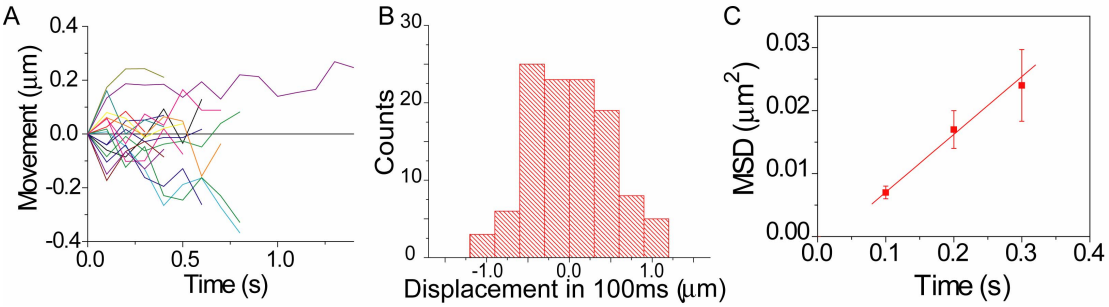

Fig. S8

6. Data analysis

Specific binding

The number of nearly diffraction limited bright spots per image frame was counted using visual inspection. In the analysis, we excluded cells for which it is unclear if there was specific binding or not. For instance, a small fraction of cell may have too high fluorescence background.

The number of bright spots was divided by the number of distinct cells per image frame (See Fig. S9). Assuming that most operator regions are bound under non-induced conditions, the probability that an operator region has a bound TF is obtained by normalizing the measured fraction by the average number of bright spots per cell observed for non-induced cells (=0.87).

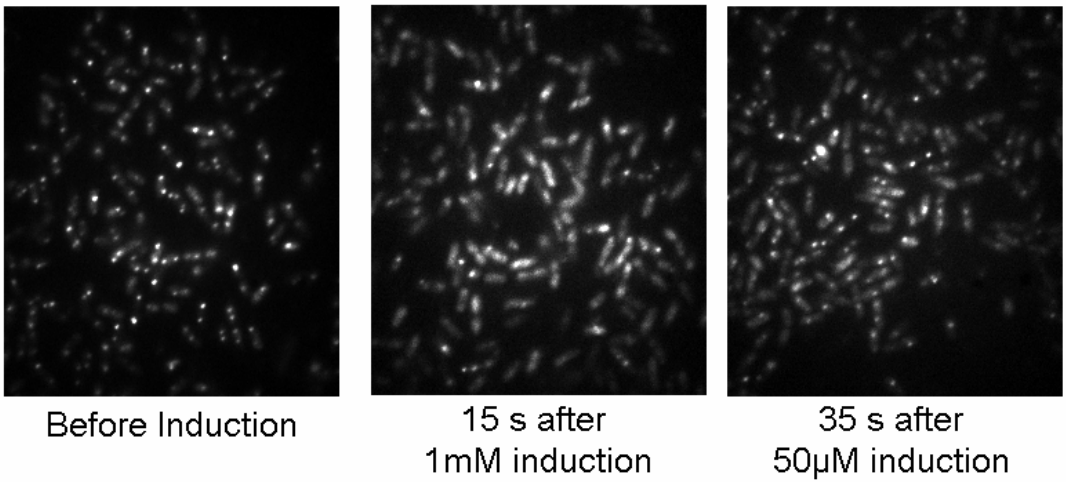

Fig. S9 Example frames before and at two time points after induction corresponding to two different points on the 1mM and 50μM induction curves in Fig. 2B

In the repression experiment where we dilute IPTG from 100 μM to 2 μM and add 1 mM ONPF, we assume that that the dissociation of IPTG from the cytoplasmic repressor is much faster than the time it takes the repressor to find the operator. The IPTG dissociation rate was measured to be 0.2 s^{-1} *in vitro* (*8*). The data for operator association is therefore fitted (Fig. 2D) with a single exponential, $a - be^{-t/T}$, where *T* corresponds to the time its takes for any of the repressors to find one of the two O1 operators. The time T is determined to be ~59 s. Considering there are approximately three dimers per *lac* operon, we estimate that it takes 59 s x 3 x 2 = ~354 s for a single repressor to find a single unoccupied *lac* operator. The error bars in Fig. 2D is determined from three different experiments.

To analyze the induction data we rely on *in vitro* experiments that have shown that the dissociation of one repressor dimer from a *lac* operator requires binding of two inducer molecules, and that it is the relatively slow association rate of the latter that determines

the rate of repressor dissociation from the operator (*9*). We further assume that the intracellular concentration of IPTG is identical to the concentration in the growth medium.

To determine the limiting IPTG association rate *in vivo*, we fit the induction data (Fig. 2B) to a model where a repressor dimer (R) dissociates from the operator (O) after binding of an IPTG molecule (I) with association rate constant k_a. The master equation that describes the probability, P(*i*, *t*), that *i* dimers are operator-bound at time *t* after induction is:

$$\begin{array}{l} OR_2 + I \xrightarrow{k_a} OR_1 + RI \\ OR_1 + I \xrightarrow{k_a} O + RI \end{array} \Leftrightarrow \left\{ \begin{array}{l} \dfrac{dP(2,t)}{dt} = -2k_a[IPTG]P(2) \\ \dfrac{dP(1,t)}{dt} = 2k_a[IPTG]P(2) - k_a[IPTG]P(1) \\ \dfrac{dP(0,t)}{dt} = k_a[IPTG]P(1) \\ P(2,0) = 1, P(1,0) = 0, P(0,0) = 0 \end{array} \right\} \qquad \text{(Eq. S1)}$$

Since we can not distinguish one operator bound dimer (OR_1) from two bound operator bound dimers (OR_2), our observable is

$$P(1,t) + P(2,t) = 1 - e^{-2k[IPTG]t}\left(e^{k[IPTG]t} - 1\right)^2 .$$

This function was fitted to the operator dissociation data (Fig 2B). To determine the mixing time of inducer in the growth media, we simultaneously fit the time interval between the pre-induction data point and the first data point after induction. The fitted association rate constant is 851 $M^{-1}s^{-1}$ and the time delay due to mixing is 2.7 s. In Fig. 2B, the data points obtained at 5s, 15s, 25s *etc*. are thus plotted at 2.3s, 12.3s, 22.3s *etc*. in order to be shown in the same graph as the fitted curves. The association rate constant k_a=851 $M^{-1}s^{-1}$ is 10-fold lower than the literature value obtained *in vitro* (*8*). The reason for this discrepancy is not clear at this point, and it could indicate that association of IPTG to the repressor is limited by the membrane permeability to IPTG.

Since the model (Eq. S1) does not consider rebinding of repressors to the operators, it can only describe the short-time kinetics before the system approaches steady state. For this reason we have also fitted the data to a model where we consider that there is equilibrium between IPTG-bound and free repressors in the cytoplasm and that the free repressors can rebind the operators. Such a model requires additional parameters that were obtained from *in vitro* measurement reported in literature (*8*). The association rate constant, k_a, is in this case estimated to be marginally higher and we can partly account for the non-zero plateau values at 50 μM. However, the major discrepancy between the model and the data is still observed for the 200 μM IPTG induction curve. It appears that a fraction (15-20%) of the cells responds slower to induction than the rest of the cells, possibly due to differences in membrane permeability.

Fluorescence spot size determination
Each fluorescent spot was fitted with a 2-dimensional Gaussian function in a 0.95 x 0.95 micron vicinity, using the in-house software GeneTrack based in Matlab (available at request). The spatial variance of each spot is determined by the fitting parameter. The average of the variances reported in Fig. 3B is an average of ~100 spots for each exposure time. For longer exposure times (>10 ms), it became more and more difficult to distinguish diffuse spots from the auto-fluorescence background under induced conditions. Only the images with comprehensible localization were selected to calculate the width, which may bias the selection of spots towards the smaller spots in each image.

Single molecule tracking and determination of the apparent 3D diffusion constant.
Positions of individual molecules are determined using commercial software, Diatrack. The software fits each fluorescent spot with a 2-dimensional Gaussian function and determines its centroid position. The spatial precision (~50 nm) is determined by the number of fluorescence photons (~100), pixel size (167 nm), and background noise (~7 photons) (*10*). Fluorescent spots in successive frames are connected by visual inspection. Care is taken to avoid selection of trajectories where two molecules come close to each other and become indistinguishable. Although each trajectory is limited to 3-4 frames due to photobleaching, we were able to derive displacement distributions for various time intervals by sampling hundreds of molecules. The displacements were recorded to calculate the mean square displacements in Fig 4C. The error bars in Fig 4C were estimated by computer simulations, in which the experiments with the same sample size were simulated 100 times and the standard error was calculated from the resultant 100 MSD values. The simulation consists of 3D random walks with 1 microsecond interval and a diffusion constant corresponding to our measured value. The net displacements were projected onto two dimensions at each time interval corresponding to our experimental timing.

Diffusive motion of facilitated target search
In this section we show that the simplest case of combined 3D and 1D motion leads to an effective normal diffusion at our experimental time scales (>10 ms). Upon comparison between the model and data, we then estimate the fraction of time that the TF spends on DNA.

First we set out by assuming that the 3D searching in the cytoplasm and the 1D sliding along DNA both display normal diffusion. We further simplify the system by assuming that the macroscopic dissociation and association to neighboring DNA segments are effectively memory-free. This allows us to model the TF motion as two diffusing species that interchange between themselves with exponentially distributed waiting times. Since the chromosomal DNA in *E. coli* can be seen as randomly oriented on our experimental length scale (>50 nm), the single-molecule reaction-diffusion master equation can be reduced to one-dimension as:

$$\frac{\partial P_1(x,t)}{\partial t} = \frac{D_1}{3}\frac{\partial^2 P_1(x,t)}{\partial x^2} + k_a P_3(x,t) - k_d P_1(x,t)$$

$$\frac{\partial P_3(x,t)}{\partial t} = D_3\frac{\partial^2 P_3(x,t)}{\partial x^2} - k_a P_3(x,t) + k_d P_1(x,t)$$

where P_1 and P_3 are the probability densities for the molecule in 1D and 3D motion, respectively. D_3 is the cytoplasmic diffusion constant. D_1 is the sliding diffusion constant, and we divide the value by three here because we project the randomly oriented DNA onto 1D. k_a is the DNA-TF association rate, and k_d is the dissociation rate.

The equation above can be solved in the Fourier-Laplace domain (*11*). The resultant mean square displacement follows a linear dependence in time. That is,

$$\left\langle \Delta x^2 \right\rangle = 2D_{eff}t,$$

where D_{eff} is defined as

$$D_{eff} = (1-f)D_3 + f\frac{D_3}{3},$$

and $f=k_a/(k_a+k_d)$ is the fraction of time that the TF spends on DNA.

We have measured the three relevant diffusion constants (Table 1) in the equation above. Considering that $0 < f < 1$, the contribution of the last term in the equation above is at most one-tenth of D_{eff}. Hence we approximate D_{eff} by

$$D_{eff} \approx (1-f)D_3.$$

In other words, the movement in the stroboscopic imaging is mostly due to 3D diffusion in cytoplasm. This allows us to estimate f, the fraction of time spent on DNA, for a given D_3. Using FCS we determined the *in vivo* diffusion rate of LacI-Venus without DNA binding domain to be $D_3 \sim 3\ \mu m^2 s^{-1}$. Therefore we estimate f to be 87% from our apparent diffusion constant $D_{eff} = 0.4\ \mu m^2 s^{-1}$.

Estimating the lower bound of nonspecific residence time

After measuring the fraction of time LacI spends on nonspecific DNA (~87%), we can predict a lower bound of the residence time based on the maximum (diffusion-limited) association rate of the two species. Consider the following mass action:

$$R + D^{ns} \xleftrightarrow{K_{RD}} R \cdot D^{ns},$$

where R represents the repressor, D^{ns} the nonspecific site, and K_{RD} the equilibrium constant. From the apparent and 3D diffusion constants, we determined

$$f \equiv \frac{[R \cdot D^{ns}]}{[R \cdot D^{ns}]+[R]} = 0.87.$$

If we rewrite the equilibrium concentrations in terms of kinetics constants, we get

$$\frac{[R \cdot D^{ns}]}{[R \cdot D^{ns}]+[R]} = \frac{[D^{ns}]K_{RD}}{1+[D^{ns}]K_{RD}}.$$

Using the same notation as in the main text, we have $[D^{ns}] \approx M/1\mu m^3 \approx 4.8 \times 10^6$ bp/μm^3. Therefore, the equilibrium binding constant is

$$K_{RD} \approx 10^3 M^{-1}.$$

Since the maximum rate of macroscopic association to nonspecific sites is limited by diffusion, the maximum dissociation rate is also limited by diffusion. At this limit, the upper bound of the macroscopic dissociation rate is (*12*)

$$\frac{1}{t_R^{\min}} \equiv k_d^{\max} \approx \frac{2\pi D_3 l}{K_{RD}},$$

where l is the length of each base pair (0.34 nm). As a result, we obtain the lower bound of the residence time

$$t_R^{\min} \approx 0.3ms .$$

From the measurement of fluorescence spot size as a function of exposure time (Fig. 3B), we determined an upper bound of the residence time to be 5 ms. Therefore the range of possible residence time *in vivo* is

$$0.3ms \le t_R \le 5ms .$$

Furthermore, the average residence time, t_c, of LacI in cytoplasm after macroscopic dissociation can be derived from the equilibrium constant and the range of residence time on DNA:

$$0.03ms \le t_C \le 0.6ms .$$

Moreover, the lower bound of the residence time on DNA provides an estimate of the lower bound in search time. As given by (Eq. 1) with t_R=0.3 ms, the minimum search time would be 65 s. The search time could be further reduced if parts of the chromosomal DNA are sequestered and inaccessible for nonspecific binding, while the operator region still is accessible. Suppose a fraction, α, of the chromosome is accessible to nonspecific binding. For a fixed f as we measured, the minimal residence time would be increased by a factor of $1/\alpha$ and the search time would be reduced by a factor of $\sqrt{\alpha}$.

References

1. A. J. Link, D. Phillips, G. M. Church, *J Bacteriol* **179**, 6228 (1997).
2. K. A. Datsenko, B. L. Wanner, *Proc Natl Acad Sci U S A* **97**, 6640 (2000).
3. S. Oehler, E. R. Eismann, H. Kramer, B. Muller-Hill, *Embo J* **9**, 973 (1990).
4. T. T. Le *et al.*, *Proc Natl Acad Sci U S A* **102**, 9160 (2005).
5. M. B. Elowitz, M. G. Surette, P. E. Wolf, J. B. Stock, S. Leibler, *J Bacteriol* **181**, 197 (1999).
6. P. C. Blainey, A. M. van Oijen, A. Banerjee, G. L. Verdine, X. S. Xie, *Proc Natl Acad Sci U S A* **103**, 5752 (2006).
7. Y. M. Wang, R. H. Austin, E. C. Cox, *Phys Rev Lett* **97**, 048302 (2006).
8. M. Dunaway *et al.*, *J Biol Chem* **255**, 10115 (1980).
9. L. Swint-Kruse, H. Zhan, K. S. Matthews, *Biochemistry* **44**, 11201 (2005).
10. R. E. Thompson, D. R. Larson, W. W. Webb, *Biophys J* **82**, 2775 (2002).
11. J. W. Haus, K. W. Kehr, *Physics Reports* **150**, 263 (1987).
12. R. B. Winter, O. G. Berg, P. H. von Hippel, *Biochemistry* **20**, 6961 (1981).

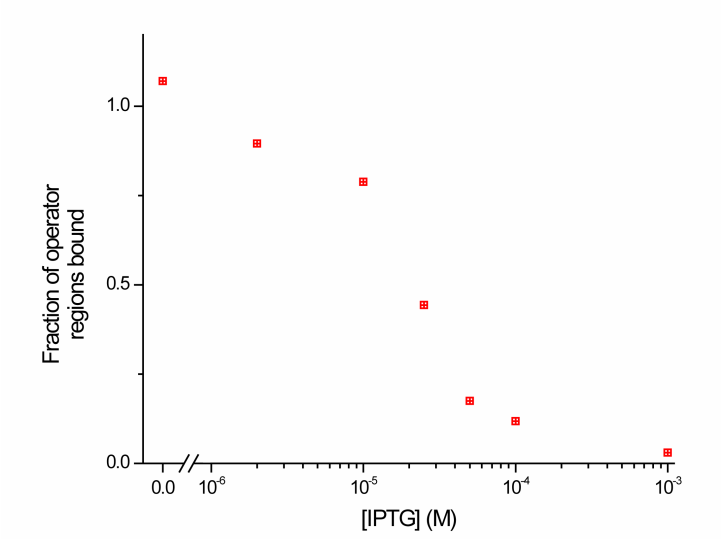

Fig. S2 Fraction of operator regions bound to LacI (*y-axis*) measured twenty minutes after addition of IPTG to different final concentrations (*x-axis*).

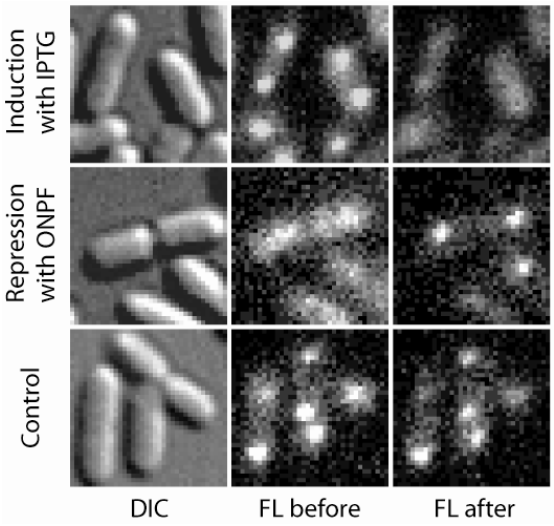

Fig. S3 Top row shows the same *JE12* bacteria before and 40sec after addition of IPTG to 1mM. Middle row shows the same *JE12* bacteria before and 1 min after dilution of IPTG from 100µM to 2µM. Bottom row shows two exposures same *JE12* bacteria without adding or removing inducer.

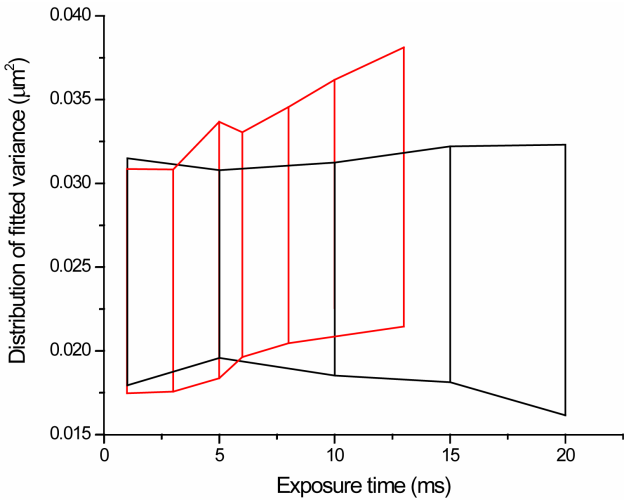

Fig. S4 Distribution of fitted spot variances at various exposure times with (*red*) and without (*black*) IPTG. The second and third quartiles of the distributions are represented by the range between the upper and lower boundaries of each vertical line. The data shows that the increase in the average spot size under induced conditions (Fig 3B) is due to that the entire distribution is shifted towards higher values.